Article:
Laurent, H, Soper, A and Dougan, L orcid.org/0000-0002-2620-5827 (2019) Biomolecular self-assembly under extreme Martian mimetic conditions. Molecular Physics, 117 (22). pp. 3398-3407. ISSN 0026-8976

https://doi.org/10.1080/00268976.2019.1649485

Biomolecular Self-Assembly Under Extreme Martian Mimetic Conditions

Harrison Laurent[1,3], Alan Soper[2], Lorna Dougan[1,3]

[1]Department of Physics and Astronomy, University of Leeds, Leeds, LS2 9JT, UK.

[2]ISIS Facility, STFC Rutherford Appleton Laboratory, Harwell, Didcot, Oxford, OX11 0QX, UK.

[3]Astbury Centre for Structural and Molecular Biology, University of Leeds, Leeds, LS2 9JT, UK.

Correspondence should be addressed to Lorna Dougan, Department of Physics and Astronomy, University of Leeds, Leeds, LS2 9JT, UK. Email: L.Dougan@leeds.ac.uk

Word count: 4067 pure text, 5750 total

Harrison Laurent ORDiD: 0000-0002-8925-4773

Biomolecular Self-Assembly Under Extreme Martian Mimetic Conditions

The recent discovery of subsurface water on Mars has challenged our understanding of the natural limits of life. The presence of magnesium perchlorate ($Mg(ClO_4)_2$) on the Martian surface raises the possibility that it may also be present in this subsurface lake. Given that the subsurface lakes on Earth, such as Lake Vostok and Lake Whillans, are capable of harbouring surprising amounts of life, these new findings raise interesting possibilities for how biomolecules might self-assemble in this environment on Mars. Here we investigate the self-association and hydration of the amino acid glycine in aqueous $Mg(ClO_4)_2$ at 25°C and -20°C using neutron diffraction with hydrogen isotope substitution and subsequent analysis with empirical potential structure refinement to yield a simulated box of atoms consistent with the scattering data. We find that although the highly chaotropic properties of $Mg(ClO_4)_2$ disrupt the hydration and hydrogen bonding ability of the amino acid, as well as the bulk water structure, glycine molecules are nonetheless still able to self-associate. This occurs more readily at lower temperature, where clusters of up to three molecules are observed, allowing us to speculate that the formation of biological molecules is possible in the Martian environment.

Keywords: neutron diffraction; empirical potential structure refinement; amino acid; water; clustering

Introduction

As our understanding of biological life on Earth has grown, we have also developed a deep interest in the solvent environment which defines biomolecules: water. Far from our initial view of water as a passive diffusive matrix for much more exciting biomolecules and biochemistry, we now know that it is an active contributor to life on every length scale [1]. Its loosely packed, hydrogen bonded, tetrahedral network of polar molecules yield a host of fascinating, and in many cases unexplained phenomena [2-4], such as its unusual density variation as a function of temperature, and its ability to

spontaneously drive unfolded proteins into functional conformations and make them the workhorses of biology [5]. It is in fact so fundamental to life, that speculations of life elsewhere in the universe are fuelled by the discovery of extra-terrestrial liquid water [6].

Over the past decade there has been growing evidence of periods of flowing surface water on Mars [7-14], and it is now known that there exists subsurface water in the form of a lake located 1.5 km below the surface near the south pole [15]. This environment may be comparable with subsurface lakes found on Earth, such as Lake Vostok and Lake Whillans, which are capable of harbouring surprising amounts of life [16-18]. The "active" Lake Whillans, underneath 800 m of ice, showed a metabolically active and diverse microbial ecosystem with 130,000 cells per millilitre of extracted lake water [17], whereas the "inactive" Lake Vostok, underneath 3800 m of ice, revealed two confirmed bacterial phylotypes, one of which was a hitherto-unknown type of bacterium referred to as W123-10.

When we start to consider the hostile environment of the subsurface Martian water, we must speculate on its likely contents. It is known that Martian soil contains magnesium perchlorate ($Mg(ClO_4)_2$) [7,10,13,14], hence it is reasonable to assume that this is also present in the subsurface water. However there exists no direct evidence of what its concentration may be. While it is shown that $Mg(ClO_4)_2$ can become highly bactericidal when irradiated by UV flux levels consistent with what would be expected at the Martian surface [19], or when desiccated [20], this subsurface briny water would offer an environment where these bactericidal effects would be significantly diminished. It has been shown that several organisms, such as the microorganism Halorubrum lacusprofundi isolated from Deep Lake in Antarctica, are capable of anaerobic growth in 0.04 M $Mg(ClO_4)_2$ [21,22], hence the presence of this salt alone does not eliminate the

possibility for life. Both ionic species in this compound are highly chaotropic and therefore act as powerful protein denaturants due to their strong interaction with the surfaces of biological molecules [23-25].

These ions also act to perturb water structure [26-29] and therefore are likely to perturb hydrogen bonding. $Mg(ClO_4)_2$ does this particularly effectively and is capable of compressing water structure in a manner similar to the formation of ice VII at room temperature, corresponding to an external pressure of approximately 3 GPa [30,31]. This phenomenon leads us to ask the question: how does the presence of $Mg(ClO_4)_2$ affect the hydration and association of biological molecules in water? This is investigated at a near eutectic [7] magnesium perchlorate concentration and using glycine as a model amino acid due to its molecular simplicity, high solubility [32], and previously recorded presence in astronomical environments [33-35]. Data was collected using neutron scattering with isotopic substitution at 25^{o}C and -20^{o}C and analysed using empirical potential structure refinement (EPSR) [36-38] to yield a simulated box of atoms consistent with the scattering data. These two temperatures were chosen as they are between the freezing temperature of eutectic NaCl solution and the bubble temperature of eutectic NH_3 solution, as these will be the subject of future investigations. It is found that while magnesium perchlorate disrupts the hydrogen bonding ability of the amino acids, they are still able to cluster, and that this clustering is temperature dependent.

Materials and Methods

Neutron Diffraction

Measurements were taken using the Near to InterMediate Range Order Diffractometer [39] (NIMROD) at the ISIS neutron facility. This covers a wide Q range of 0.1-300 nm^{-1}, where Q is the difference in momentum between the incident and scattered neutrons,

corresponding to interatomic separations of 0.1-30 nm. The obtained data can then be used to yield the total interference differential scattering cross section, $F(Q)$, which can then be broken down into its constituent partial structure factors $S(Q)$ [30,36]. The relative contribution of each partial structure factor to the total structure factor is dependent on the particular atomic species' concentration c, and their nuclear scattering length b, such that:

$$F(Q) = \sum_{\alpha\beta} c_\alpha c_\beta b_\alpha b_\beta \left(S_{\alpha\beta}(Q) - 1\right) \quad (1)$$

The Fourier transform of the partial structure factor then gives the corresponding RDF, the integral of which then yields the corresponding coordination numbers. Data were corrected for multiple scattering, attenuation, and inelastic scattering using Gudrun software.

Sample Densities

Densities of final samples were measured by weighing 1 mL of sample. The results were then verified by using a densitometer. It was also assumed that the densities of the samples containing both $Mg(ClO_4)_2$ and glycine changed negligibly at lower temperatures. The densities were then calculated in terms of atoms/$Å^3$, and the final values of 0.0975 and 0.1030 atoms/$Å^3$ for the samples with and without $Mg(ClO_4)_2$ respectively were applied to the EPSR simulations.

EPSR Simulations

In order to perform EPSR analysis, a cubic simulation box was built such that the experimental concentrations, temperatures, and densities were matched (Supplementary Table 1). The EPSR simulations of the pure water and glycine samples contained 172 glycine molecules and 5160 water molecules in a cubic box of dimension 55.0677 Å at 25^{o}C, yielding an atomic number density of 0.1030 atoms/$Å^3$. The simulations of the

samples containing $Mg(ClO_4)_2$ contained 172 glycine molecules, 5418 water molecules, 325 Mg^{2+} ions and 650 ClO_4^- ions in a cubic box of dimension 60.4608 Å at 25°C and -20°C, yielding an atomic number density of 0.0975 atoms/Å^3. Glycine was modelled in its zwitterionic form which occurs in solution at neutral pH [40]. The $Mg(ClO_4)_2$ concentration used here corresponds to 39.6 wt%, which is near the eutectic concentration of 44 wt% [7]. The experiment was originally designed such that a eutectic concentration of $Mg(ClO_4)_2$ would be used, however due to the highly hydroscopic properties of $Mg(ClO_4)_2$, it is likely that H_2O was absorbed into the chemical from the atmosphere before the final samples were made. Therefore the final concentration of $Mg(ClO_4)_2$ was determined from the predicted differential scattering cross section of the neutron scattering data. This can be considered a reliable way of verifying the concentration as the predicted differential scattering cross section is extremely sensitive to hydrogen isotope substitution due to their large differences in scattering lengths. All bond lengths, angles, Lennard Jones and Coulomb parameters of all components were set to match values found in literature [30,41-48] (Supplementary Table 2). As no previous neutron diffraction and EPSR analysis based literature exists documenting the Lennard Jones or Coulomb parameters of glycine this was estimated from neutron diffraction experiments of other amino acids and short peptides. Freindorf et al. [49] used a combined DFT quantum mechanical and AMBER molecular mechanical potential approach to determine the Lennard Jones parameters for the atomic species present in several amino acids and compared these to the results found using other potentials. The results are in good agreement with the σ values, however the ε are much lower than those used in this research. There is also a large contrast with the values determined for hydrogen, as it is typically modelled in EPSR such that it only interacts via a Coulomb force. All final parameters can be found in the supplementary

information, as well as the final fits for $F(Q)$ from the EPSR simulations (Supplementary figures 10-12). It is important to note that the resultant EPSR simulations do not guarantee unique molecular positions and orientations that perfectly match the samples, but merely solutions that are consistent with the scattering data and are based on sensible interaction parameters. The divergence of the EPSR simulated fits to the data at low Q values are a result of insufficient correction of the data to account for inelasticity effects, which becomes increasingly difficult at low Q values and with samples containing large quantities of light atoms, such as hydrogen. It is highly unlikely however to impact the overall structure observed from the resulting EPSR [50].

Results

Local Water Structure

The EPSR analysis yields the partial structure factors, and hence radial distribution functions (RDFs), for all interatomic correlations. Perturbation to water structure can be discussed in terms of the water oxygen – water oxygen (O_wO_w) and the water oxygen – water hydrogen (O_wH_w) RDFs as shown in Supplementary Figures 1 and 2, their coordination numbers, and visualised using spatial density functions (SDFs). Distances used to calculate the coordination numbers can be found in Supplementary Tables 3a-c. Upon the addition of glycine, the water structure undergoes a slight perturbation as the first peak in the O_wO_w RDF shifts slightly inwards from 2.82 Å in the case of ambient water [2] to 2.79 Å. The O_wH_w peaks still occur either side of the O_wO_w peak at 1.86 and 3.35 Å respectively. The second hydration shell is drawn inwards from ~4.5 Å in the case of ambient water [2,51,52] to 4.42 Å in glycine solution. This slight compression is also reflected by an increase of the height of the first peak in the O_wO_w RDF from 2.49 in the case of ambient water [2] to 2.98 while decreasing the O_wO_w average

coordination number found in ambient water of ~4.7 to 4.167±0.005, where the quoted uncertainty for all coordination numbers reported in this paper are calculated by fitting a Gaussian peak to the coordination numbers predicted from EPSR using Origin 9.1. This yields an uncertainty associated with the position of the centre of the peak. A reduction of this coordination number, together with the compression effects observed within the RDF suggest that the observed decrease in this coordination number is due to an excluded volume effect of the glycine. The O_wH_w average coordination number in the case of ambient water is given as 1.88 [2], whereas the current research finds 2.378±0.007 when calculated over near identical distances. This striking increase is particularly significant as this coordination number is associated with hydrogen bonding in water, and will be explored in more detail in the discussion section. Two hydration shells are also clearly visible in the SDF shown in figure 2. The similarity of this SDF to ambient water, together with the similarity of the O_wO_w coordination number, RDF peak heights and their positions, suggest that the water is relatively structurally unperturbed, and therefore the hydrogen bond network is likely to remain mostly intact.

As with previous results [30], in the presence of $Mg(ClO_4)_2$ a highly compressed structure emerges with the second hydration shell collapsing into the first, as can also be seen in figure 1, and the third hydration shell being drawn inwards from 6.93 to 5.39 and 5.00 Å at 25^{o}C and -20^{o}C respectively. Hydration shell collapse is reflected by an increased O_wO_w coordination number of 5.635±0.006 and 5.841±0.004 at 25 and -20^{o}C respectively. Despite the large structural perturbation, the O_wH_w peak positions do not change significantly, but the coordination numbers decrease slightly to 1.947±0.002 and 1.718±0.004 at 25 and -20^{o}C respectively. This implies that the hydrogen bonding network is perturbed to a lesser degree than the overall structural perturbation would suggest, as has been seen previously in molecular dynamics simulation studies [51].

Glycine Hydration

As would be expected, glycine is strongly hydrated around the hydrophilic amine and carbonyl groups. In the absence of $Mg(ClO_4)_2$, each amine hydrogen (H_x) coordinates an average of 0.9034±0.0001 water oxygens at a distance of 1.78 Å. Each carbonyl oxygen (O_1) coordinates 3.230±0.005water oxygens at a distance of 2.67 Å, and 2.52±0.01 water hydrogens at a distance of 1.70 Å. The average O_1O_w and O_1H_w coordination numbers suggest that 78% of the coordinated water molecules orient an OH bond toward the carbonyl oxygen at a slightly shorter than those found in bulk water. Upon addition of $Mg(ClO_4)_2$ a slight compression of the first hydration shell is seen around the carbonyl oxygen, with the O_1H_w distance being drawn into 1.74 and 1.69 Å at 25 and -20^{o}C respectively. Around the amine hydrogen the peak position does not change significantly in the first hydration shell, but the second hydration shell is drawn inwards from 3.22 to 3.12 Å at -20^{o}C. The structural perturbation is reflected in the average O_1O_w coordination number (Supplementary Tables 3b and c). This is shown to decrease to 2.484±0.005 at 25^{o}C and increase to 3.952±0.002 at -20^{o}C, while the O_1H_w coordination number is shown to decrease to 0.4±0.2 and 1.2±0.5 at 25 and -20^{o}C respectively. The large discrepancy between the O_1O_w average coordination numbers in the presence of $Mg(ClO_4)_2$ is likely due to the relatively large difference between the distances used to calculate the coordination numbers, as shown in supplementary tables 3a-c. The intensity of the first peaks in these OH RDFs also decrease for both the amine and carbonyl groups in the presence of $Mg(ClO_4)_2$, with the -20^{o}C peak having higher intensity than the 25^{o}C (Supplementary figure 3 and 4 respectively). The zwitterionic nature of the modelled glycine also means there is charge ordering of the magnesium ion around the carbonyl group and the perchlorate ion around the amine group as evidenced by the relevant RDFs (Supplementary figures 13 and 14 respectively). The

peaks observed in both RDFs decrease in intensity with decreasing temperature due to preferential hydrogen bonding of the amine and carbonyl groups to the surrounding water molecules resulting in a decrease in association between the charged amine and carbonyl groups and the ions. The O1Mg RDF features an intense sharp peak centred at 1.48 Å, which is reminiscent of a chemical bond. However this is unrealistic for our system and likely a result of the large charge difference between the Mg^{2+} ion and the carbonyl oxygen.

Glycine Association

Using EPSR it is also possible to estimate glycine cluster formation. In this work two molecules are deemed clustered if one of their amine hydrogens is within a given distance of the neighbouring glycine's carbonyl oxygen. This distance corresponds to the first minimum of the relevant O_1H_x RDF (Supplementary figure 6). This method of evaluating clustering will be explained further in the discussion section. The cluster size distribution is shown in figure 3, where the largest cluster size predicted through EPSR is three glycine molecules in the case of aqueous glycine, and the proportion of molecules found in clusters of two or more molecules is 0.320. It is clear that while the presence of $Mg(ClO_4)_2$ is hindering clustering by screening the charge based interactions, as the proportion of molecules found in clusters of two or more molecules decreases to 0.203 and 0.221 at 25^{o}C and -20^{o}C respectively , it is not destroying it completely. A temperature dependence is therefore observed for the clustering in the samples containing $Mg(ClO_4)_2$, with clusters of two glycine molecules occurring 17% less frequently at the lower temperature, and clusters of three glycine molecules occurring over 4 times more frequently. This is also reflected by the relative intensities of the first and second peaks in the O_1H_x RDF, where the pure glycine and water sample has the highest intensity for both the first and second peak. Both samples containing

$Mg(ClO_4)_2$ have identical first peak heights, however the second peak is significantly higher for the lower temperature sample, as shown in supplementary figure 6.

Discussion

Bulk Water Structure

In this research the O_wH_w average coordination number was shown to increase in the presence of glycine compared to ambient water while an excluded volume effect of the glycine simultaneously decreased the O_wO_w coordination number. This suggests an increased tendency of the OH bond to orient itself towards a neighbouring water oxygen which could be interpreted as an increase in bulk water hydrogen bonding. The ratio of the two coordination numbers suggests over half of the average coordinated water molecules have their OH bonds oriented towards the central molecule and are acting as hydrogen bond donors. This therefore predicts that the central molecule is over-bonded, with ~4.8 hydrogen bonds per molecule, and more water molecules than are predicted to be in the first hydration shell are hydrogen bonded to the central molecule. This is clearly impossible. As ambient water has somewhere between 3.4 and 3.6 hydrogen bonds per molecule [4,54-56], this increase in coordination number and the slight second hydration shell compression is likely a reflection of weakened hydrogen bonding in the bulk water with some bonds becoming too bent to still be classified as hydrogen bonds. However due to the overall similarity between pure water and water in the presence of glycine as determined by RDFs and SDFs (Figure 1 and Supplementary figure 1 and 2), and the difference between the O_wO_w peak position and the O_wH_w peak position of 0.93 nm, which is very close to the accepted OH distance found in a water molecule [43], the fraction of hydrogen bonded water molecules is likely to be mostly intact when compared with ambient water.

Hydrogen Bonding in Glycine

Aqueous amino acids and chemicals featuring similar chemical groups have been previously studied through several means, including molecular dynamics simulations and neutron diffraction studies [44-48,57-66]. These studies have consistently shown a strong hydrogen bonding ability of the hydrophilic areas of amino acid molecules, in this case the carbonyl hydrogen bond acceptor and amine hydrogen bond donor groups of glycine. It has also been shown that of the two groups the carbonyl group has a stronger hydrogen bonding capacity, with each CO group capable of forming hydrogen bonds with two water molecules compared to each NH group being capable of forming a hydrogen bond with a single water molecule. Waters bound to the carbonyl group are also reported to exhibit much slower reorientation times by a factor of ~2 compared with bulk water or water bound to the amine group. This difference in hydrogen bonding is supported by the current research. The SDFs shown in figure 2 demonstrate a clear ability of these charged groups to coordinate water molecules with each amine group usually coordinating a single water molecule and each carbonyl usually coordinating three, with some water molecules being shared between each carbonyl oxygen. This is also reflected in the relevant RDFs between the amine hydrogens or carbonyl oxygens with the water oxygens and water hydrogens. (Supplementary figures 3, 4 and 9). In both the amine and carbonyl group the hydrogen bond acceptor-donor distance is shorter than that found in bulk water with the relevant O-H distance occurring at 1.78 and 1.70 Å respectively. Here the shorter distance of the carbonyl hydrogen bond, together with a stronger first peak in the RDF, is an indicator of stronger hydrogen bonding. This is likely explained by the increased dipole moment of the CO bond. In this simulation there is a larger absolute charge difference between carbonyl carbon and oxygen compared with the amine hydrogen nitrogen (Supplementary table 2) and a greater separation between the two atoms.

Glycine molecules are therefore capable of hydrogen bonding to one another, as has been shown for other amino acids and similar molecules. Several studies [44-48,64] have now shown that hydrophilic interactions are the dominant force that drives the clustering of amino acids in solution. The most relevant example from previous literature uses L-proline [45] at a similar concentration to this research, and also finds that it typically forms dimers in solution as a result of interactions between its CO_2^- and NH_2^+ groups. This is clearly evidenced in this research. If one considers the RDF between the hydrophilic amine hydrogens and carbonyl oxygens, it is possible to assess hydrophilic association, and if one considers the RDF between the hydrophobic hydrogen side chains (H_{bk}) it is possible to assess hydrophobic association. Comparing these two RDFs, as shown in figure 4, it is clear that the O_1H_x has clear maxima and minima implying a reoccurring structural motif, whereas the $H_{bk}H_{bk}$ has no significant discernible features. This suggests that any clustering of glycine molecules is driven by hydrophilic forces rather than hydrophobic. It is possible to verify this hydrophilic association by running the EPSR simulation in the absence of glycine atomic charges. If the clustering was occurring as a result of hydrophobic effects then this would still occur with glycine molecules with no partial charges, however clustering is almost entirely eliminated with 97.6, 98.8 and 95.1% of glycine molecules existing as monomers for aqueous glycine at 25^{o}C, and glycine in aqueous $Mg(ClO_4)_2$ at 25 and -20^{o}C respectively. (Supplementary Figure 5). The observed temperature dependence on cluster size distribution also suggests an enthalpic origin for the hydrophilic interaction between glycine molecules. An enhanced level of clustering is therefore indicative of increased hydrogen bonding between glycine molecules at lower temperatures. This is consistent with previous studies on water – alcohol solutions [67-69] and is consistent with hydrogen bonding in liquid water [4,70,71]. Whilst it is difficult to comment on the

directionality of the bond formed between amine and carbonyl groups of neighbouring glycine molecules, and hence to what extent this is a true hydrogen bond, there are several consistencies between the observed affects and what would be predicted through hydrogen bonding.

Magnesium Perchlorate

As described in the Results section, the addition of $Mg(ClO_4)_2$ perturbs bulk water structure, glycine hydration, and glycine clustering. A slight compression of the hydration shell around both hydrophilic areas of the glycine molecule is observed. This is more apparent for the carbonyl group where the first peak in the O_1O_w RDF shifts inwards and decreases in size and the associated coordination number changes significantly while the O_1H_w coordination number simultaneously decreases. These effects are less apparent at lower temperature. Collectively, this indicates that $Mg(ClO_4)_2$ acts to reduce the hydrogen bonding ability of the amine and carbonyl groups with the surrounding water, likely by screening the charge based hydrophilic interactions. It is also evident from the coordination numbers and relative first OH peak intensities that hydrogen bonding is preserved to a greater extent at lower temperature. This is clear when comparing the SDFs shown in figure 2, where the hydration structure around both charged groups in the presence of $Mg(ClO_4)_2$ is more reminiscent of pure water and glycine at lower temperature. This is consistent with previous results, as an increased hydrogen bonding ability of hydrophilic groups within larger molecules at lower temperatures has been observed in neutron diffraction experiments on aqueous methanol and ethanol [4,67-69]. The reduction in hydrogen bonding ability of the glycine by $Mg(ClO_4)_2$ would also explain the observed reduction in glycine clustering and the associated temperature dependence.

As glycine is the simplest amino acid, it is likely that the perturbations to clustering by $Mg(ClO_4)_2$ shown in this work would occur for all zwitterionic amino acids. It is also likely that an amino acid with a charged side chain would resist this perturbation to a greater extent by offering a site for preferential association of the ions, and thus protecting the hydrogen bonding ability of the amine and carbonyl group. It is certainly true that salt-loving halophilic organisms tend to have a higher concentration of charged amino acids on the surface of their proteins, and that these are likely to help screen the effect of the ions present in their solvent environment and therefore preserve the hydrogen bonding network present of the protein. At a larger scale the effect of $Mg(ClO_4)_2$ on the viability of mesophilic and halophilic organisms has been tested with mixed results [19-22,72]. Some organisms experience a rapid decrease in viability, while some are unaffected, and some are even capable of anaerobic growth in 40 mM $Mg(ClO_4)_2$. The perturbation but ultimate persistence of hydrogen bonding in the extreme case of near eutectic $Mg(ClO_4)_2$ studied here, combined with the ability of some terrestrial organisms to thrive at low $Mg(ClO_4)_2$ concentrations, seems to suggest that the limits to life are not met by the mere presence of this highly chaotropic salt.

Acknowledgements

The project was supported by a grant from the Engineering and Physical Sciences Research Council (EPSRC) (EP/P020088X/1) to Dr L. Dougan. Harrison Laurent is jointly supported by an EPSRC DTA studentship and an ISIS Facility Development Studentship. Experiments at the ISIS Pulsed Neutron Facility were supported by a beam time allocation from the Science and Technology Facilities Council under proposal number RB 1800054. The authors thank Tristan Youngs for his support during the running of the neutron diffraction experiments.

Declaration of Interest

The authors declare no competing interests

References

[1] P. Ball, Proc. Natl. Acad. Sci. **114**, 13327 (2017).

[2] A. K. Soper, ISRN Phys. Chem. **2013**, 1 (2013).

[3] K. Amann-Winkel, M.C. Bellissent-Funel, L.E. Bove, T. Loerting, A. Nilsson, A. Paciaroni, D. Schlesinger, and L. Skinner, Chem. Rev. **116**, 7570 (2016).

[4] L. Zhao, K. Ma, and Z. Yang, Int. J. Mol. Sci. **16**, 8454 (2015).

[5] M.C. Bellissent-Funel, A. Hassanali, M. Havenith, R. Henchman, P. Pohl, F. Sterpone, D. Van Der Spoel, Y. Xu, and A.E. Garcia, Chem. Rev. **116**, 7673 (2016).

[6] E.F. van Dishoeck, E.A. Bergin, D.C. Lis, and J.I. Lunine, in Protostars Planets VI (2014).

[7] V.F. Chevrier, J. Hanley, and T.S. Altheide, Geophys. Res. Lett. **36**, L10202 (2009).

[8] F.J. Martín-Torres, M.-P. Zorzano, P. Valentín-Serrano, A.-M. Harri, M. Genzer, O. Kemppinen, E.G. Rivera-Valentin, I. Jun, J. Wray, M. Bo Madsen, W. Goetz, A.S. McEwen, C. Hardgrove, N. Renno, V.F. Chevrier, M. Mischna, R. Navarro-González, J. Martínez-Frías, P. Conrad, T. McConnochie, C. Cockell, G. Berger, A. R. Vasavada, D. Sumner, and D. Vaniman, Nat. Geosci. **8**, 357 (2015).

[9] A.S. McEwen, L. Ojha, C.M. Dundas, S.S. Mattson, S. Byrne, J.J. Wray, S.C. Cull, S.L. Murchie, N. Thomas, and V.C. Gulick, Science (80-.). **333**, 740 (2011).

[10] S.C. Cull, R.E. Arvidson, J.G. Catalano, D.W. Ming, R. V Morris, M.T. Mellon, and M. Lemmon, Geophys. Res. Lett. **37**, L22203 (2010).

[11] J.D. Rummel, D.W. Beaty, M.A. Jones, C. Bakermans, N.G. Barlow, P.J. Boston, V.F. Chevrier, B.C. Clark, J.-P.P. de Vera, R. V Gough, J.E. Hallsworth, J.W. Head, V.J. Hipkin, T.L. Kieft, A.S. McEwen, M.T. Mellon, J.A. Mikucki, W.L. Nicholson, C.R. Omelon, R. Peterson, E.E. Roden, B. Sherwood Lollar, K.L. Tanaka, D. Viola, and J.J. Wray, Astrobiology **14**, 887 (2014).

[12] G.M. Marion, D.C. Catling, K.J. Zahnle, and M.W. Claire, Icarus **207**, 675 (2009).

[13] J.D. Toner, D.C. Catling, and B. Light, Geochim. Cosmochim. Acta **136**, 142 (2014).

[14] M.H. Hecht, S.P. Kounaves, R.C. Quinn, S.J. West, S.M.M. Young, D.W. Ming, D.C. Catling, B.C. Clark, W. V. Boynton, J. Hoffman, L.P. DeFlores, K. Gospodinova, J. Kapit, and P.H. Smith, Science (80-.). **325**, 64 (2009).

[15] R. Orosei, S.E. Lauro, E. Pettinelli, A. Cicchetti, M. Coradini, B. Cosciotti, F. Di Paolo, E. Flamini, E. Mattei, M. Pajola, F. Soldovieri, M. Cartacci, F. Cassenti, A. Frigeri, S. Giuppi, R. Martufi, A. Masdea, G. Mitri, C. Nenna, R. Noschese, M. Restano, and R. Seu, Science (80-.). **361**, 490 (2018).

[16] D. Fox, Nature **512**, 244 (2014).

[17] B.C. Christner, J.C. Priscu, A.M. Achberger, C. Barbante, S.P. Carter, K. Christianson, A.B. Michaud, J.A. Mikucki, A.C. Mitchell, M.L. Skidmore, T.J. Vick-Majors, W.P. Adkins, S. Anandakrishnan, S. Anandakrishnan, L. Beem, A. Behar, M. Beitch, R. Bolsey, C. Branecky, A. Fisher, N. Foley, K.D. Mankoff, D. Sampson, S.

Tulaczyk, R. Edwards, S. Kelley, J. Sherve, H.A. Fricker, S. Siegfried, B. Guthrie, T. Hodson, R. Powell, R. Scherer, H. Horgan, R. Jacobel, E. McBryan, and A. Purcell, Nature **512**, 310 (2014).

[18] S.A. Bulat, Philos. Trans. R. Soc. A Math. Phys. Eng. Sci. **374**, (2016).

[19] J. Wadsworth and C.S. Cockell, Sci. Rep. **7**, 4662 (2017).

[20] K. Beblo-Vranesevic, M. Bohmeier, A.K. Perras, P. Schwendner, E. Rabbow, C.S. Moissl-Eichinger, Christine, Cockell, R. Pukall, P. Vannier, V.T. Marteinsson, E.P. Monaghan, P. Ehrenfreund, L. Garcia-Descalzo, F. Gomez, M. Malki, R. Amils, F. Gaboyer, F. Westall, P. Cabezas, N. Walter, and P. Rettberg, PLoS One **12**, (2017).

[21] V.J. Laye and S. DasSarma, Astrobiology **18**, 412 (2017).

[22] A. Oren, R. Elevi Bardavid, and L. Mana, Extremophiles **18**, 75 (2014).

[23] N. Schwierz, D. Horinek, U. Sivan, and R.R. Netz, Curr. Opin. Colloid Interface Sci. **23**, 10 (2016).

[24] A.H. Crevenna, N. Naredi-Rainer, D.C. Lamb, R. Wedlich-Söldner, and J. Dzubiella, Biophys. J. **102**, 907 (2012).

[25] H.I. Okur, J. Hladílková, K.B. Rembert, Y. Cho, J. Heyda, J. Dzubiella, P.S. Cremer, and P. Jungwirth, J. Phys. Chem. B **121**, 1997 (2017).

[26] K.D. Collins, G.W. Neilson, and J.E. Enderby, Biophys. Chem. **128**, 95 (2007).

[27] K. Ma and L. Zhao, Int. J. Mol. Sci. **17**, (2016).

[28] M.Y. Kiriukhin and K.D. Collins, Biophys. Chem. **99**, 155 (2002).

[29] R. Mancinelli, A. Sodo, F. Bruni, M.A. Ricci, and A.K. Soper, J. Phys. Chem. B **113**, 4075 (2009).

[30] S. Lenton, N.H. Rhys, J.J. Towey, A.K. Soper, and L. Dougan, Nat. Commun. **8**, 1 (2017).

[31] W.F. Kuhs, J.L. Finney, C. Vettier, and D. V. Bliss, J. Chem. Phys. **81**, 3612 (1984).

[32] R. Carta and G. Tola, J. Chem. Eng. Data **41**, 414 (1996).

[33] H. Cottin, J.M. Kotler, K. Bartik, H.J. Cleaves, C.S. Cockell, J.P.P. de Vera, P. Ehrenfreund, S. Leuko, I.L. Ten Kate, Z. Martins, R. Pascal, R. Quinn, P. Rettberg, and F. Westall, Space Sci. Rev. **209**, 1 (2017).

[34] O. Botta and J.L. Bada, Surv. Geophys. **23**, 411 (2002).

[35] K. Altwegg, H. Balsiger, A. Bar-Nun, J.J. Berthelier, A. Bieler, P. Bochsler, C. Briois, U. Calmonte, M.R. Combi, H. Cottin, J. De Keyser, F. Dhooghe, B. Fiethe, S.A. Fuselier, S. Gasc, T.I. Gombosi, K.C. Hansen, M. Haessig, A. Jäckel, E. Kopp, A. Korth, L. Le Roy, U. Mall, B. Marty, O. Mousis, T. Owen, H. Rème, M. Rubin, T. Sémon, C.Y. Tzou, J.H. Waite, and P. Wurz, Sci. Adv. **2**, (2016).

[36] A.K. Soper, Phys. Rev. B **72**, 104204 (2005).

[37] A.K. Soper, Mol. Phys. **99**, 1503 (2001).

[38] A.K. Soper, Chem. Phys. **202**, 295 (1996).

[39] D.T. Bowron, A.K. Soper, K. Jones, S. Ansell, S. Birch, J. Norris, L. Perrott, D. Riedel, N.J. Rhodes, S.R. Wakefield, A. Botti, M.A. Ricci, F. Grazzi, and M. Zoppi, Rev. Sci. Instrum. **81**, 033905 (2010).

[40] S. Roy, A. Hossain, K. Mahali, and B.K. Dolui, Russ. J. Phys. Chem. A **89**, 2111 (2015).

[41] P.-G. Jonsson and A. Kvick, Acta Cryst. **B28**, 1827 (1972).

[42] H.K. Lim, Y.S. Choi, and S.T. Hong, Acta Crystallogr. Sect. C Cryst. Struct. Commun. **67**, i36 (2011).

[43] A.G. Császár, G. Czakó, T. Furtenbacher, J. Tennyson, V. Szalay, S. V. Shirin, N.F. Zobov, and O.L. Polyansky, J. Chem. Phys. **122**, 214305 (2005).

[44] E. Scoppola, A. Sodo, S.E. McLain, M.A. Ricci, and F. Bruni, Biophys. J. **106**, 1701 (2014).

[45] S. Busch, C.D. Lorenz, J. Taylor, L.C. Pardo, and S.E. Mclain, J. Phys. Chem. B **118**, 14267 (2014).

[46] N.H. Rhys, A.K. Soper, and L. Dougan, J. Phys. Chem. B **116**, 13308 (2012).

[47] S.E. McLain, A.K. Soper, and A. Watts, Eur. Biophys. J. **37**, 647 (2008).

[48] S.E. McLain, A.K. Soper, I. Daidone, J.C. Smith, and A. Watts, Angew. Chemie - Int. Ed. **47**, 9059 (2008).

[49] M. Freindorf, Y. Shao, T.R. Furlani, and J. Kong, J. Comput. Chem. **26**, 1270 (2005).

[50] F. Meersman, D. Bowron, A.K. Soper, and M.H.J. Koch, Biophys. J. **97**, 2559 (2009).

[51] A.K. Soper and M.A. Ricci, Phys. Rev. Lett. **84**, 2881 (2000).

[52] A.H. Narten and H.A. Levy, Science (80-.). **165**, 447 (1969).

[53] S. Imoto, H. Forbert, and D. Marx, Phys. Chem. Chem. Phys **17**, 24224 (2015).

[54] R. Kumar, J.R. Schmidt, and J.L. Skinner, J. Chem. Phys. **126**, 204107 (2007).

[55] D. Swiatla-Wojcik, Chem. Phys. **342**, 260 (2007).

[56] B.M. Auer and J.L. Skinner, Chem. Phys. Lett. **470**, 13 (2009).

[57] F. Sterpone, G. Stirnemann, J.T. Hynes, and D. Laage, J. Phys. Chem. B **114**, 2083 (2010).

[58] D. Russo, G. Hura, and T. Head-Gordon, Biophys. J. **86**, 1852 (2004).

[59] C. Malardier-Jugroot, D.T. Bowron, A.K. Soper, M.E. Johnson, and T. Head-Gordon, Phys. Chem. Chem. Phys. **12**, 382 (2010).

[60] I. Daidone, C. Iacobucci, S.E. McLain, and J.C. Smith, Biophys. J. **103**, 1518 (2012).

[61] S. Busch, L.C. Pardo, W.B. O'Dell, C.D. Bruce, C.D. Lorenz, and S.E. McLain, Phys. Chem. Chem. Phys. **15**, 21023 (2013).

[62] S. Busch, C.D. Bruce, C. Redfield, C.D. Lorenz, and S.E. McLain, Angew. Chemie - Int. Ed. **52**, 13091 (2013).

[63] N. Steinke, R.J. Gillams, L.C. Pardo, C.D. Lorenz, and S.E. Mclain, Phys. Chem. Chem. Phys. Phys. Chem. Chem. Phys **18**, 3862 (2016).

[64] N.H. Rhys, A.K. Soper, and L. Dougan, J. Phys. Chem. B **119**, 15644 (2015).

[65] S.E. Norman, A.H. Turner, and T.G.A. Youngs, RSC Adv. **5**, 67220 (2015).

[66] S. Biswas and B.S. Mallik, J. Mol. Liq. **212**, 941 (2015).

[67] S. Lenton, N.H. Rhys, J.J. Towey, A.K. Soper, and L. Dougan, J. Phys. Chem. B **122**, 7884 (2018).

[68] L. Dougan, S.P. Bates, R. Hargreaves, J.P. Fox, J. Crain, J.L. Finney, V. Réat, and A.K. Soper, J. Chem. Phys. **121**, 6456 (2004).

[69] L. Dougan, R. Hargreaves, S.P. Bates, J.L. Finney, V. Ŕat, A.K. Soper, and J. Crain, J. Chem. Phys. **122**, 174517 (2005).

[70] C. Huang, K.T. Wikfeldt, D. Nordlund, U. Bergmann, T. McQueen, J. Sellberg, L.G.M. Pettersson, and A. Nilsson, Phys. Chem. Chem. Phys. **13**, 19997 (2011).

[71] L. Xu, F. Mallamace, Z. Yan, F.W. Starr, S. V Buldyrev, and H.E. Stanley, Nat. Phys. **5**, 565 (2009).

[72] A.H. Stevens, D. Childers, M. Fox-Powell, N. Nicholson, E. Jhoti, and C.S. Cockell, Astrobiology ast.2018.1840 (2018).

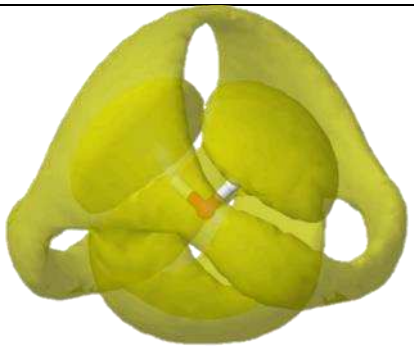

Water 25°C

Aqueous $Mg(ClO_4)_2$ 25°C

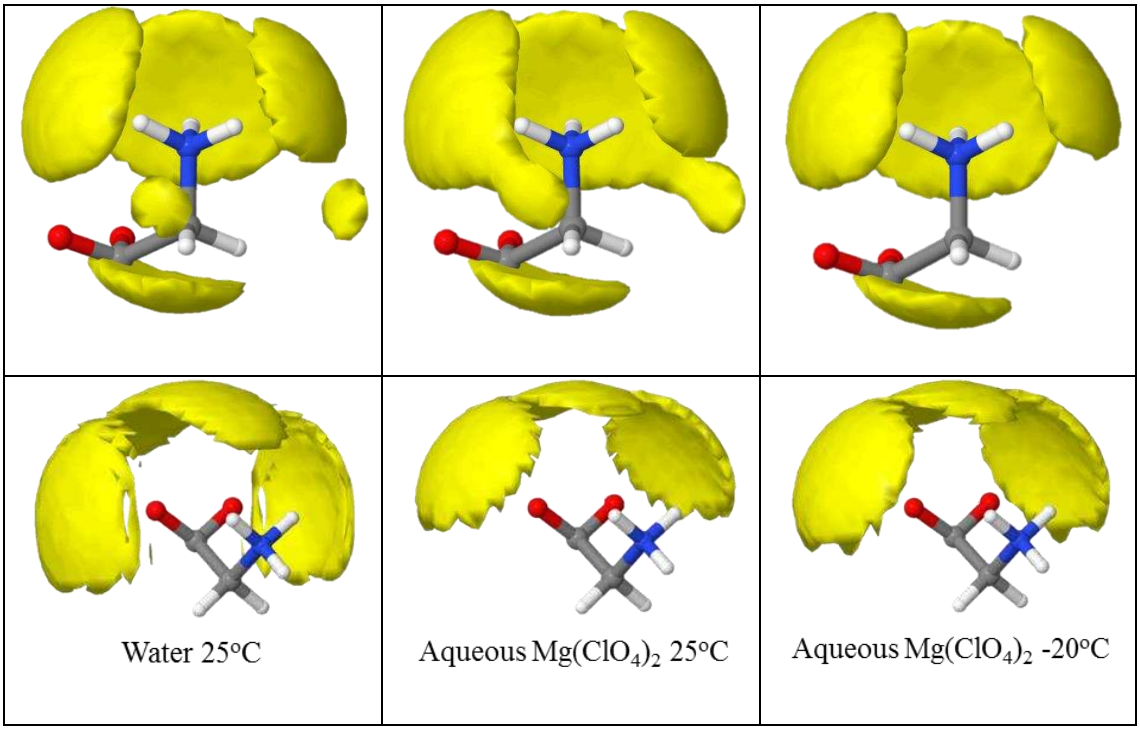

Water 25°C | Aqueous $Mg(ClO_4)_2$ 25°C | Aqueous $Mg(ClO_4)_2$ -20°C

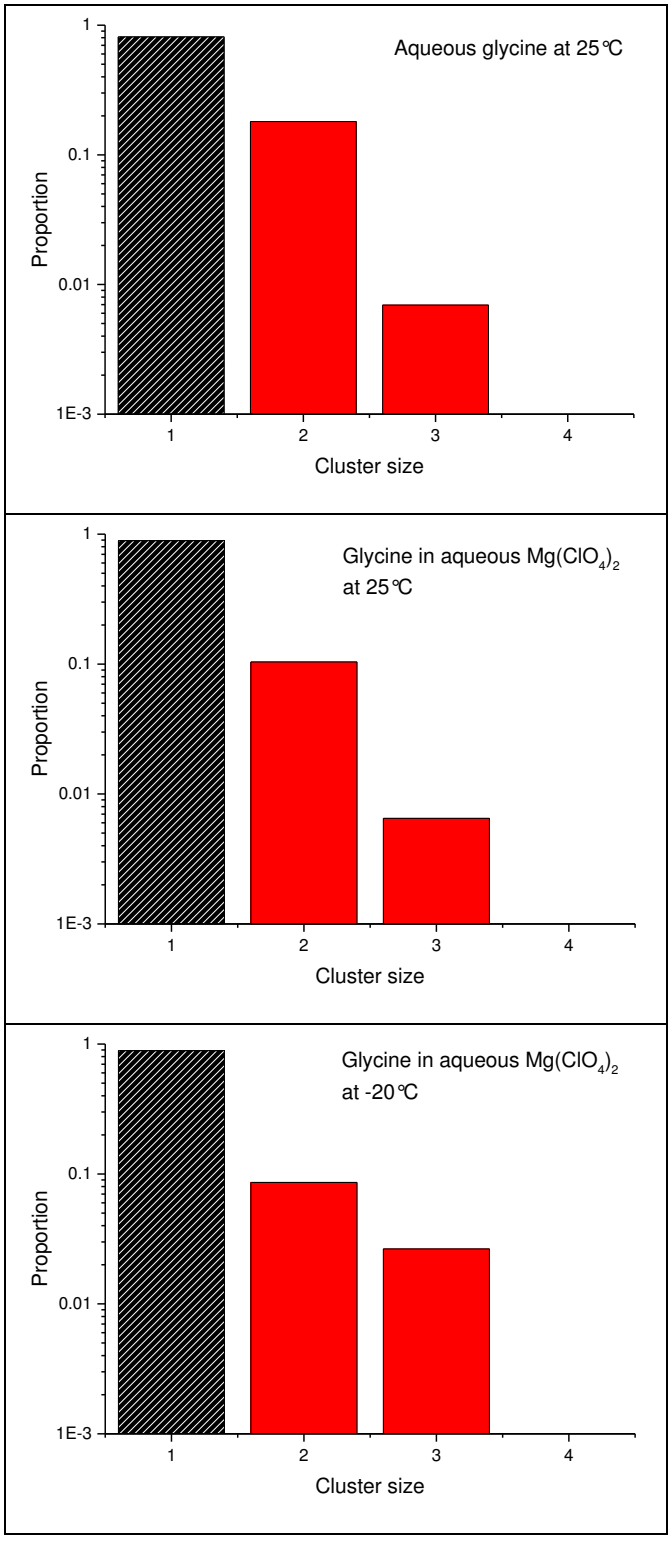
Aqueous glycine at 25℃
Proportion
1
0.1
0.01
1E-3
1
2
3
4
Cluster size
Glycine in aqueous Mg(ClO4)2
at 25℃
Proportion
1
0.1
0.01
1E-3
1
2
3
4
Cluster size
Glycine in aqueous Mg(ClO4)2
at -20℃
Proportion
1
0.1
0.01
1E-3
1
2
3
4
Cluster size

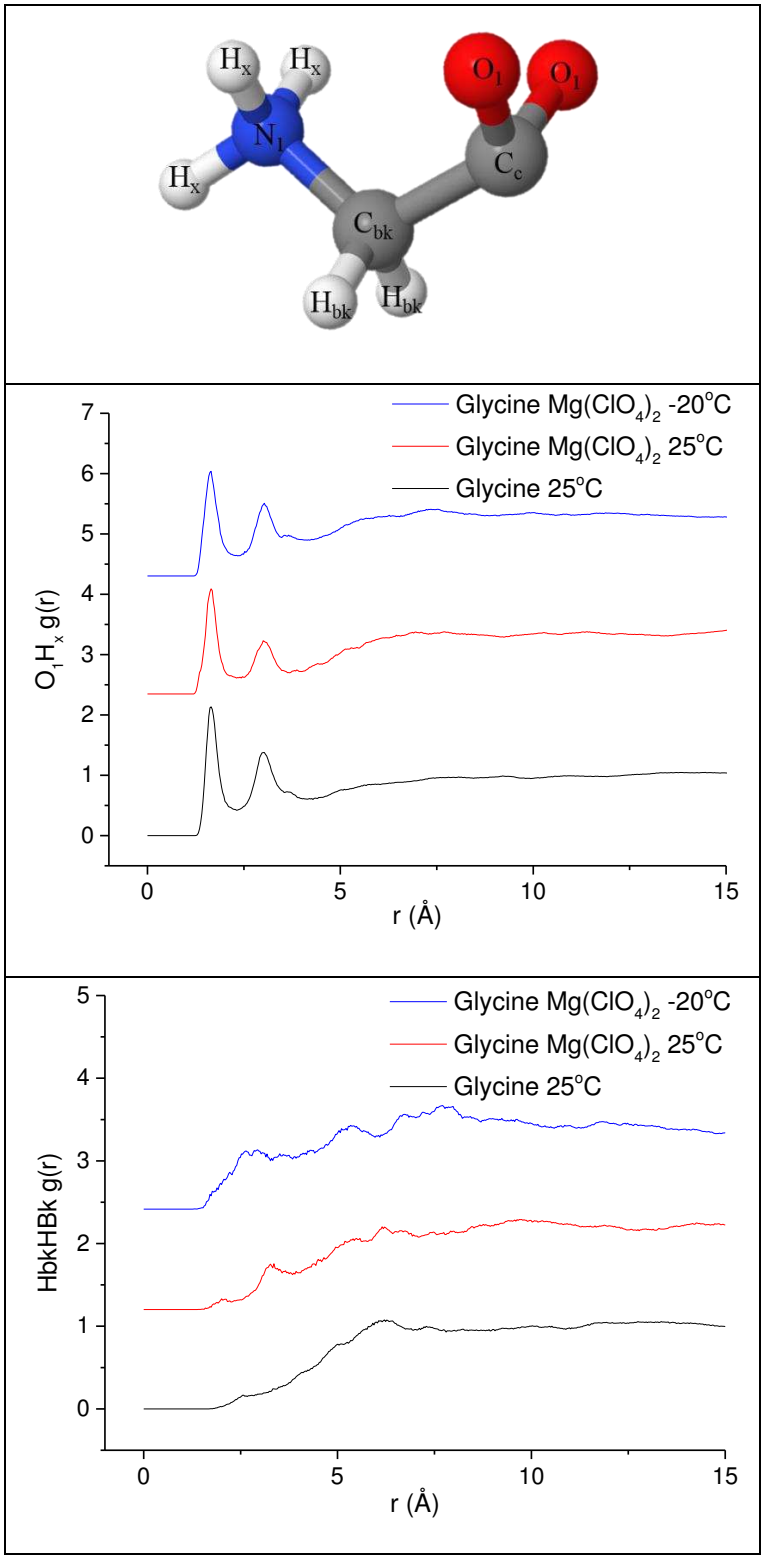
H_x
H_x
N_1
H_x
O_1
O_1
C_c
C_bk
H_bk
H_bk
Glycine Mg(ClO4)2 -20°C
Glycine Mg(ClO4)2 25°C
Glycine 25°C
O1Hx g(r)
r (Å)
Glycine Mg(ClO4)2 -20°C
Glycine Mg(ClO4)2 25°C
Glycine 25°C
HbkHBk g(r)
r (Å)

Figure 1. Spatial density functions of water around a central water molecule from neutron diffraction data and EPSR analysis for water in the presence of glycine (top) and water in the presence of glycine and Mg(ClO4)2. These surface contours contain the highest 30% probability areas of finding another molecule within a distance of 5 Å from the central molecule. (Figure updated)

Figure 2. Spatial density functions of water around a central amine group (top) or a central carbonyl group (bottom) of glycine without Mg(ClO4)2 at 25^{o}C (left), with Mg(ClO4)2 at 25^{o}C (middle), and with Mg(ClO4)2 at -20^{o}C (right) from neutron diffraction data and EPSR analysis. These surface contours contain the highest 15% probability areas of finding a water molecule within a distance of 5 Å from the central molecule. (Figure updated)

Figure 3. Cluster size distribution predicted from EPSR simulations as determined using the definition for hydrophilic clustering found in the "glycine association" section. Distribution plotted on a logarithmic scale to highlight differences in cluster size distributions. Proportion of clusters containing only one glycine molecule shown in black and white.

Figure 4. Labelling convention for glycine molecule used in present research (top). EPSR simulated RDFs of amine hydrogens from a carbonyl oxygen (middle) and side chain hydrogens from a side chain hydrogen (bottom). Spectra are vertically offset for clarity. (Figure updated)